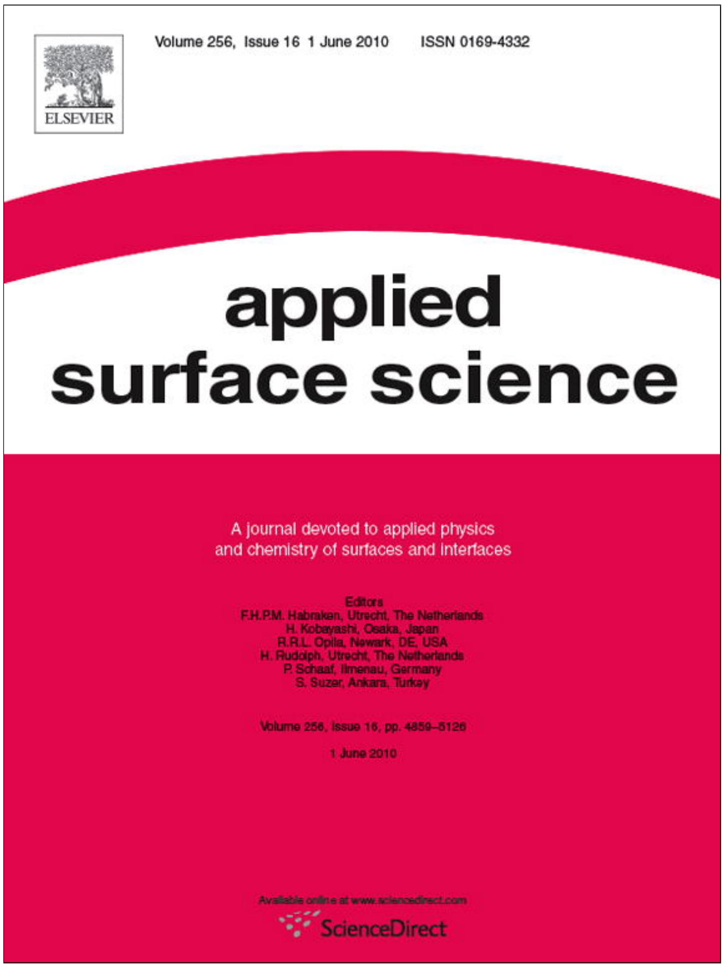
Volume 256, Issue 16 1 June 2010 ISSN 0169-4332
ELSEVIER
applied
surface science
A journal devoted to applied physics
and chemistry of surfaces and interfaces
Editors
F.H.P.M. Habraken, Utrecht, The Netherlands
H. Kobayashi, Osaka, Japan
R.R.L. Opila, Newark, DE, USA
H. Rudolph, Utrecht, The Netherlands
P. Schaaf, Ilmenau, Germany
S. Suzer, Ankara, Turkey
Volume 256, Issue 16, pp. 4859–5126
1 June 2010
Available online at www.sciencedirect.com
ScienceDirect

Applied Surface Science 256 (2010) 4990–4994

Contents lists available at ScienceDirect

Applied Surface Science

journal homepage: www.elsevier.com/locate/apsusc

Field emission pressure sensors with non-silicon membranes

N. Badi [a,b,*], A.M. Nair [a], A. Bensaoula [b]

[a] Center for Advanced Materials (CAM), University of Houston, Houston, TX 77204-5004, United States
[b] Physics Department, University of Houston, Houston, TX 77204-5005, United States

ARTICLE INFO

Article history:
Received 20 October 2009
Received in revised form 4 February 2010
Accepted 3 March 2010
Available online 16 March 2010

Keywords:
Pressure sensor
Electron field emission
Boron nitride
COMSOL multiphysics

ABSTRACT

We report on the fabrication of cold cathode emitter and the design parameter simulation of a functional field emission-based pressure sensor. This device comprises a membrane made of metallic compound acting as the anode in front of a flat cold cathode emitter. First, the mechanical deflection of a diaphragm under selected input pressures is modeled. The current density distribution in the deflected diaphragm is then calculated using realistic field emission characteristics from fabricated sulfur doped boron nitride (S-BN) cold cathode device. The total current output was found by integrating the measured current density of the fabricated electron emitter device over the entire diaphragm area of the membrane as function of external pressure. The results show that conventional silicon membranes would pose problems when implemented in a real field emission device, and show how the use of unconventional materials (i.e., TiN) can help overcome these problems.

1. Introduction

Electron field emission is a phenomenon that has been used recently in several applications, such as displays, scanning electron microscopy, and sensors [1,2]. Pressure sensors based on various field emitters have been studied and several modeling and experimental results have been reported [3–8]. Pressure sensor configurations are invariably based on the bending of a flexible membrane. When a pressure differential is applied to a membrane it bends. In field emission-based pressure sensors, the membrane acts as an anode put in front of a cold cathode emitter; its bending is sensed by measuring a change in the current collected by the membrane because of the change in electrical field between the anode and the cathode.

The above-mentioned device has significant advantages over conventional capacitive sensors (which integrate the change of elementary capacitive areas) and piezoresistive sensors (which take the difference of the resistance changes of the bridge arms). Field emission sensors are temperature insensitive and are expected to have higher thermal tolerance than commercially available sensors. They are also MEMS compatible on silicon, and the signal conditioning circuitry required is significantly simpler than the bridge circuits required by other sensors. Unlike other pressure sensors, the sensitivity of field emission pressure sensors can be increased even if the deflection of the membrane is small. This is because the electron field emission is governed by the well-known Fowler–Nordheim equation (FN), which is put into an exponential transfer function between the deflection and current density [9]. However, the exponential nature of this function also causes extensive non-linearity in the output of the device, if conventional materials like silicon are used for the device membrane.

The basic purpose of this study is to define experimental and design parameters for the fabrication of a functional field emission-based pressure sensor. This work focuses on the use of nitride materials for making sensors and how such materials would help enhance the performance of these devices. The present paper will establish that the use of stiffer metals or metallic compounds for the membrane enhance the performance of the device as compared to conventional silicon membranes.

2. Principle

A pressure sensitive electron field emitter consists of a sealed evacuated cavity between a flexible membrane (anode) and an electron field emitter, which act as the cathode. A cross section representation is shown in Fig. 1. The sensor fabrication flow chart is illustrated in Fig. 2. Titanium nitride (TiN) membrane is formed across over a deposited aluminum (Al) sacrificial layer. Al is taken off using hot HCl. The surfaces are then cleaned prior to sealing the microsensor. This can be done by using TiN evaporation at a grazing incidence angle to seal the edge of the cavity under vacuum ($<10^{-7}$ Torr). The S-BN electron emitter layer is inert in hot HCl solvent that washes off the Al sacrificial layer. The separation between TiN membrane and S-BN is determined by taking into account the

* Corresponding author at: Center for Advanced Materials (CAM), University of Houston, 724, Science & Research Bldg. 1, Houston, TX 77204-5004, United States. Tel.: +1 713 743 3621; fax: +1 713 747 7724.
E-mail address: nbadi@uh.edu (N. Badi).

0169-4332/$ – see front matter © 2010 Elsevier B.V. All rights reserved.
doi:10.1016/j.apsusc.2010.03.014

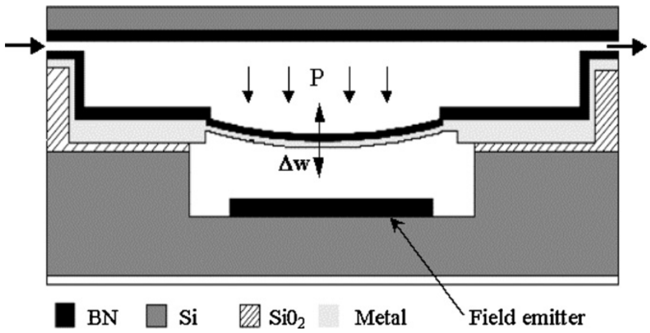

Fig. 1. Schematic cross-section of field emission pressure sensor.

thicknesses of the Al sacrificial layer, oxide, and etched S-BN film. The TiN membrane can be covered with a protective BN layer for corrosion resistance purpose. Finally, a BN coated silicon channel is bonded on the top to form the field emitter-based pressure sensor.

The process of electron field emission is based on a phenomenon in which materials emit electrons in vacuum when they are subjected to an electric field. In general, the electron field emission process takes place under strict vacuum conditions and is governed by the following FN equation:

$$J = AE^2 \exp\left[-\frac{B\phi^{3/2}}{E}\right] \quad (1)$$

In Eq. (1), J represents the current density due to the electron collection, E represents the applied electric field, ϕ represents the work function of the emitter material and A and B are numeric constants. The electric field is $E = V/d$, where V is the voltage applied between the anode and the cathode and d is the separation between them. When pressure changes the separation between the anode and the cathode, there is a change in the electric field and therefore a change in the electrical current collected by the membrane.

In our simulation we have used experimental data from a fabricated sulfur doped boron nitride (S-BN) field emitter because of its high chemical and mechanical stability under poor vacuum conditions, as high as 0.1 mTorr [10]. Among the many different parameters that govern the range and sensitivity of these pressure sensors are: geometry of the membrane, dimensions, thickness, and emitter to collector separation. The choice of membrane material is very important because materials such as commonly used silicon in conventional pressure sensors, would not only cause extreme non-linearity in the output of the field emission-based device but also drastically limit its dynamic range.

In order to design a device for a particular pressure range and with the necessary sensitivity it is essential that we know how each of the above-mentioned parameters affects the dynamic range and sensitivity of the device.

3. Gated field emitter fabrication and characterization

A 0.35 μm thick S-BN field emitter was deposited on highly conductive silicon (1 0 0) substrates at 450 °C by ion beam assisted physical vapor deposition technique (IBAD). The S-BN film was considered smooth enough with an RMS roughness of 1.0 nm. High purity boron was evaporated by electron beams and controlled by a quartz crystal rate monitor at a rate of 0.2 Å/s. The residual pressure was around 10^{-8} Torr; the pressure during film growth was around 10^{-6} Torr; mostly nitrogen from the source. Nitrogen species were delivered by a gridless End Hall ion source (Commonwealth Scientific Mark II) fed with high purity nitrogen. For sulfur doping we used a 10/90% gas mixture of compressed H_2S/N_2. A second nitrogen line was used in conjunction with the first one in order to reach the desirable S/N_2 combination ratio for controllable sul-

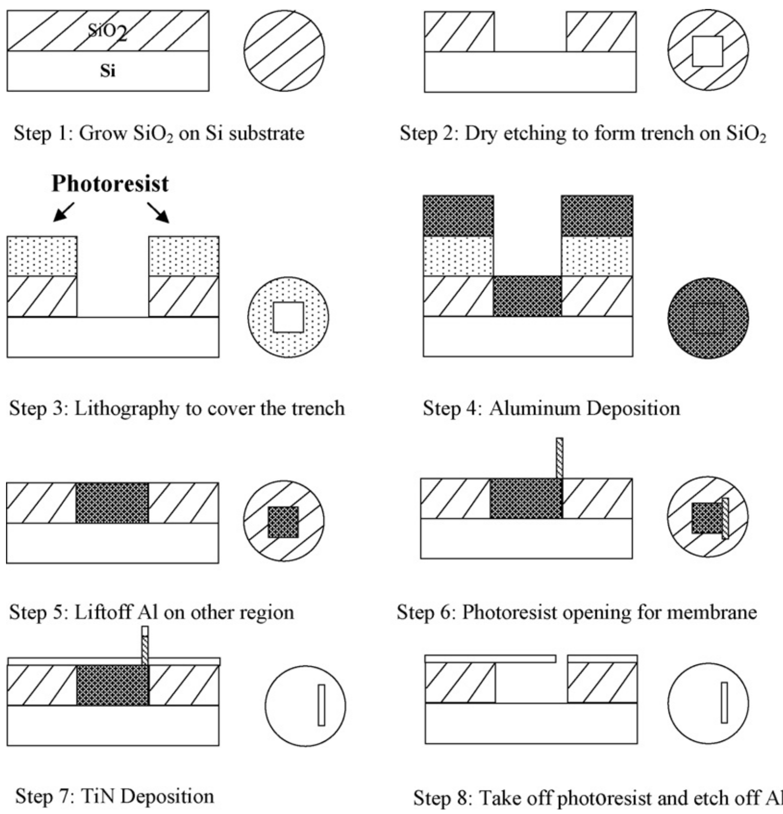

Fig. 2. Fabrication flow chat for TiN membrane fabrication using aluminum as sacrificial layer material. The sealing of the emission sites from the atmosphere is not shown here. Proposed final product will have closed cavity achieved via silicon fusion bonding.

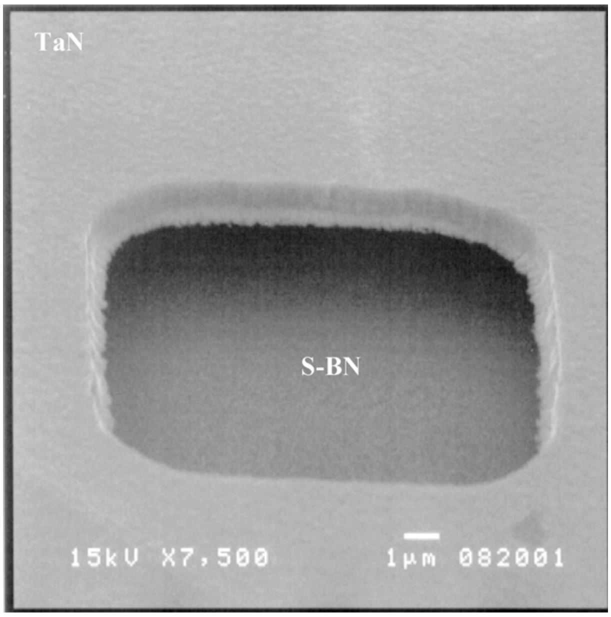

Fig. 3. TaN/SiO_2/S-BN/Si field emitter gated structure.

fur incorporation and optimum growth conditions. The sulfur as a dopant was introduced through the inlet of the ion source to generate the nitrogen/sulfur species. The sulfur concentration within the BN layer was of the order of $10^{18}/cm^3$. A 1.0 μm thick silicon dioxide layer used as a spacer between the S-BN cathode and the metallic gate was deposited at 200 °C using plasma enhanced chemical vapor deposition. The gate is made out of 1 μm thick tantalum nitride (TaN) material, which is deposited at room temperature using IBAD technique. We patterned a typical ~150 μm^2 planar gated emitters in square shape. TaN gate was dry-etched under Cl_2/Ar chemistry using plasma reactive ion etching process followed with the oxide wash-off in a HF:H_2O standard solution. The etch rates per minute for TaN and the oxide layers were about 500 Å and 4.5 μm, respectively. The SEM picture of the processed field emission gated structures shows a well-shaped undercut, smooth surface morphology, and flake-free material (Fig. 3).

Field emission characteristics were studied in a high vacuum chamber with a pressure below 10^{-7} Torr. The voltage is applied between a flat-ended tungsten tip and the film surface, with the tip–surface distance being varied between 10 and 100 μm. An XYZ stepper motor stage is used to control the tip motion in 3 directions. An optical telescope system with a CCD camera and monitor are used for monitoring tip positioning, and for immediate *in situ* observation of any electrical field induced modification of the sample surface. A high dc voltage of up to 8 kV is applied between the sample and the probe to induce field emission. The measurement procedure included recording of the emission current during the automated cycling of applied electrical fields. The emission current density was calculated by dividing the measured current by the total surface area of the used tip. Fig. 4 shows the field emission characteristics of the fabricated gated structure. The turn-on electrical field is about 60 V/μm at a maximum current density of 2.75 mA at 70 V/μm. The inset graph shows the Fowler–Nordheim fit of the field emission data indicating that the current collected indeed has field emission characteristics.

4. Modeling

Existing modeling results on field emission pressure sensors [3–5] are mainly based on membranes made from conventionally used materials like silicon and aluminum and on numerical models

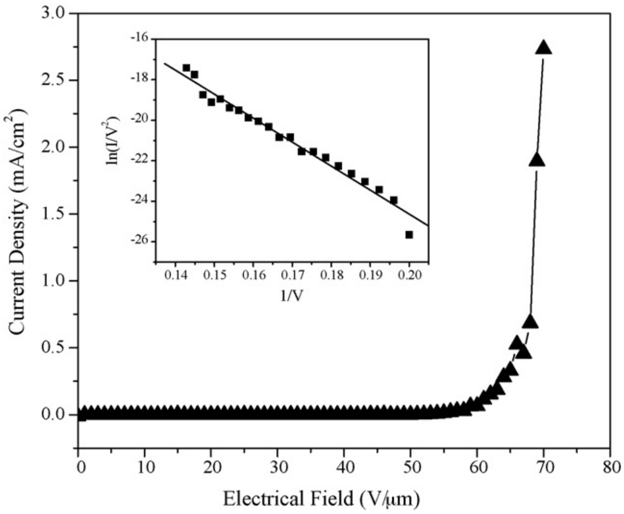

Fig. 4. Field emission characteristics and FN linear fit from a S-BN gated structure.

of field emission [11]. All these modeling results attempt to solve the problem of a membrane fixed on all sides that is described by a partial differential equation (PDE):

$$D_x \frac{\partial^4}{\partial x^4} d + 2(D_1 + 2D_{xy}) \left(\frac{\partial^2}{\partial x^2} \frac{\partial^2}{\partial w^2} d \right) + D_y \frac{\partial^4}{\partial y^4} d = P \qquad (2)$$

In Eq. (2), D_x, D_y, D_{xy} and D_1 are the flexural rigidity along different directions given in terms of the elastic modulus, shear modulus, Poisson ratio, and the thickness of the membrane. But in the case of amorphous materials they are all equal and are given in terms of the Young's modulus; w is the deflection of the membrane; and the x and y subscripts denote the directions of the applied pressure P. The solution to the above-mentioned PDE could be obtained in the analytical form. The solution is an infinite series and therefore requires an approximation. Reports have been made of applying the solution to the PDE using different numbers of terms in the infinite series. The above equation has an elementary limitation: it holds good only for small deflections; i.e. only when the deflection of the membrane is smaller than the thickness of the membrane. Also analytical methods are less accurate than finite element methods (FEM) when compared with experimental results [12].

The commercially available COMSOL software package was used to obtain the results presented in this work. The simulation is supported by data collected experimentally from materials and geometries being tested by the authors. The sensor geometry was defined as a simple shell element having an area equal to the membrane area, with all its edges fixed. This geometry was meshed with 2778 triangular elements containing 1448 nodes. The thickness and material properties, such as the Young's modulus, Poisson ratio, density, etc., were entered depending on the material for which the simulation was performed. Loads were applied on one boundary and the problem was solved to get the deflection of the membrane. A parametric solver was used to solve the problem with the applied load as the varying parameter. The electric field was determined as a function of the applied voltage and displacement of the membrane.

The constants A and B used in Eq. (1) are determined from the field emission characteristics of the S-BN gated structure shown in Fig. 4. A function was defined for the current density based on the electric field and the constants A and B. The current density was integrated over the entire boundary to get the total current collected by the device. This current was plotted versus the pressure to get the characteristics of the device. Widely available material

Table 1
Material parameters used in the simulation.

	Modulus of elasticity (E) (GPa)	Density (ρ) (Kg/m^3)	Poisson ration (ν)
Si	131	2330	0.27
Ta	186	16650	0.34
Ti	116	4507	0.32
TiN	600	5430	0.25

parameters such as modulus of elasticity, density, and Poisson ratio used for the simulation are given in Table 1.

5. Results and discussion

The simulations were first performed on a circular silicon membrane. The area and thickness of the membrane are 500 μm^2 and 3 μm, respectively. The anode to cathode separation is 3 μm and the range of applied pressures is 0–10 kPa. Membranes with minimum side length and thickness of 1 mm and 4 μm, respectively, were used for modeling a pressure sensor using a diamond field emitter [13]. Related results show an overall pressure domain shifting toward higher pressures when the square membrane side length becomes smaller; and that better sensor sensitivity is obtained for thinner membranes with smaller dimensions.

Fig. 5 shows the displacement of the membrane under a pressure of 10 kPa. The deflection of the center of the membrane at 10 kPa is 1.38 μm. Fig. 6 shows the displacement of a square membrane having an area of 500 μm^2 square and a thickness of 3 μm for the same applied pressure. The central displacement is 1.79 μm for a pressure of 10 kPa. The pressure–current characteristics of these devices are shown in Fig. 7. The characteristics show that the output of the device is extremely non-linear with changing pressure. This is undesirable because it makes the calibration and external circuitry complex. It is, however, obvious from Fig. 7 that a square membrane has a larger output current than a circular one.

The reason for this non-linear behavior is due to the fact that, for this range of pressures, the membrane causes the electrical field between the anode and the cathode to sweep over a large part of the FN curve. But if the deflection is restricted then the change in the electrical field can be limited to a smaller part of the FN curve thereby reducing the non-linearity. The deflection of the membrane can be reduced by changing the dimensions of the membrane or by changing the material that the membrane is made of.

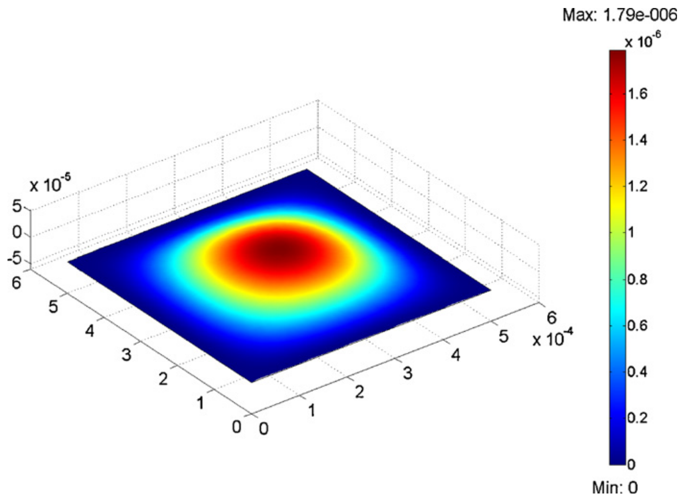

Fig. 6. Deflection of square silicon membrane at 10 kPa.

Hereunder we have investigated different materials for the membrane that give the best performance for a given geometry and dimensions. The basic requirement for the membrane is that it be made of conductive material. Since silicon membranes had non-linear characteristics, we need to use a material that deflects less than silicon for the given pressure, so that their deflections will be smaller and the characteristics will sweep over a smaller part of the FN curve. This implies that the material needs to have a higher modulus of elasticity than silicon. The materials that were tried are titanium, tantalum and titanium nitride.

Fig. 8 shows the pressure–current characteristics of devices having titanium, tantalum, and titanium nitride membranes. We see that the titanium-based device is more non-linear as compared to silicon. This is because titanium has a lower Young's modulus than silicon. The tantalum membrane has significantly more linear characteristics than the silicon and titanium membrane. We also see a marked drop in the current output of the tantalum device as compared to the silicon-based device. This is expected because the deflection of the membrane from its null position is small. The characteristics of the titanium nitride membranes are almost a straight line, with an output current of 3.1 μA at 10 kPa. The entire range of output current over the entire 10 kPa is only about 1.25 μA. This renders the device unusable because of extremely low sensitivity. For the TiN membrane with an emitter–collector separation

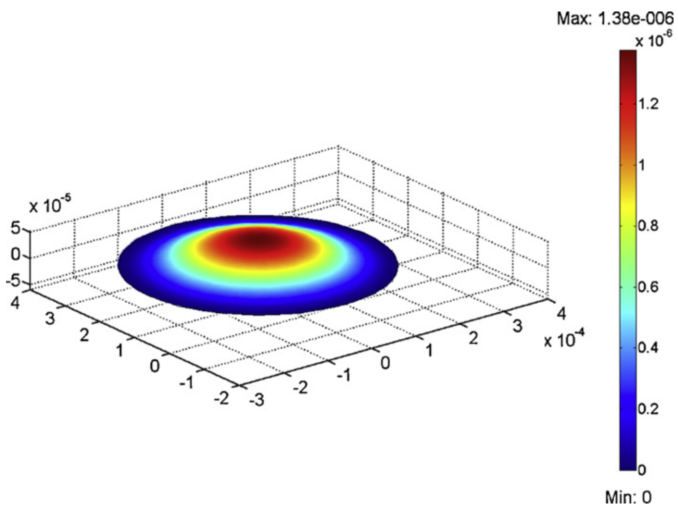

Fig. 5. Deflection of circular silicon membrane at 10 kPa.

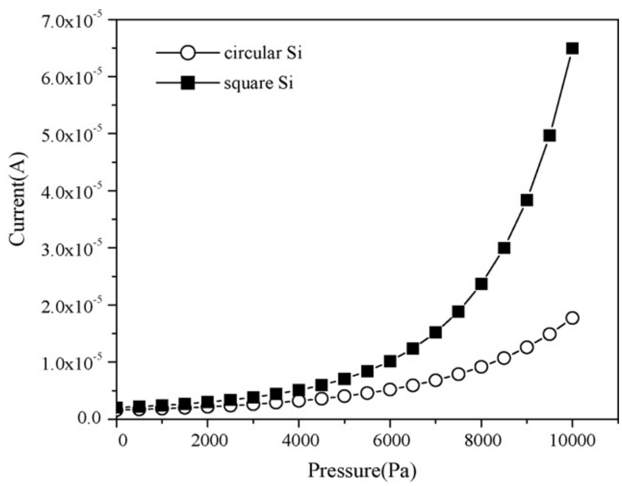

Fig. 7. Pressure–current characteristics of circular and square silicon membranes.

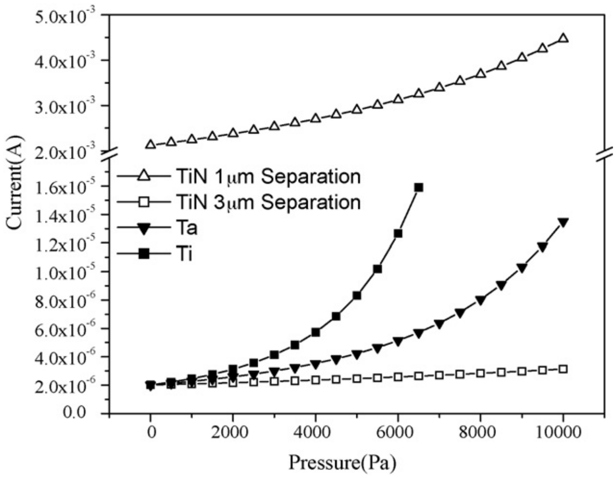

Fig. 8. Pressure–current characteristics of Ti, Ta, and TiN membranes.

of 1 μm, the operating current regime of the device increases by 3 orders of magnitude and the linearity of the device is maintained.

Generally speaking it is preferable that a sensor displays a constant sensitivity over the range of values it is designed to measure. The sensitivity of the Si and Ti devices is found to vary extensively over the pressure range. The tantalum based device's sensitivity doesn't change that much. However, while the sensitivity of the TiN based device is practically constant over the pressure range, it is extremely low and is therefore unusable. The reason for this, as mentioned previously, is that since the deflection of the TiN membrane from its null position even at 10 kPa is only about 0.4 μm, the electrical field change is thus very small. This problem can be solved either by increasing the voltage applied to the device or by reducing the emitter–collector separation. Since increasing the voltage is not a desirable option the best choice is to reduce the emitter–collector separation. Such an approach is only possible if the field-emitting cathode is extremely flat. This is one of the key advantages of our BN materials [14,15], which pocesses a very smooth surface morphology and therefore tolerate much shorter cathode to anode separation, characteristics not achievable when using traditional Si field emitter tips.

6. Conclusion

We simulated the performance of field emission-based pressure sensors having membranes made of silicon and metallic compounds. Results show that while simple and reliable field emission devices can be designed to yield extremely sensitive pressure sensors, their characteristics are critically dependent on the type of material in use as well as on its specific geometry. It is apparent from the simulation results that square membranes have better current output when compared to circular ones of equal area. Silicon membranes, commonly used in capacitive and piezoresitive pressure sensors, may not be applicable for field emission-based pressure sensors. The simulated sensor behavior of such devices is unusable because of their non-linearity. This non-linearity, which is inherent to the device because of its exponential transfer function, i.e. the FN equation, can be greatly reduced by using stiffer membranes that would deflect less under a given pressure thus causing the output to sweep over a smaller part of the FN curve. The choice of material is therefore critical to the performance of the device. Of the materials investigated, TiN seems to have the most desirable characteristics with respect to linearity. This is because of their small deflection. But this small deflection also causes a loss in the sensitivity of the device.

Changing the emitter–collector separation can make up for the loss in sensitivity, because of the small deflection. Changing the emitter–collector separation causes the electrical field to vary within a higher regime of the FN equation. However, the sweep is still over a small portion of the FN curve because of the corresponding small deflection. This causes the sensitivity to rise without affecting the linearity of the device. The results obtained from the simulation could be further used to improve sensor design and also be of interest to people trying to fabricate field emission-based pressure sensors. We wish to simulate the dynamic range of the present pressure sensor and how the sensitivity of the device would change in different pressure ranges. The effect of the membrane area and thickness on the dynamic range and sensitivity, as well as the effect of residual stress due to multilayer films structure on device performance, will also be reported.

Acknowledgements

This material is based upon work supported by the National Science Foundation under Grant No. 0010100 and the NASA cooperative agreement to the University of Houston Center for Advanced Materials (CAM).

References

[1] J. Dijon, A. Fournier, T. Goislard De Mosabert, B. Montmayeul, D. Zanghi, AIP Conf. Proc. 685 (2003) 592.
[2] D. Nicolescu, V. Filip, J. Itoh, Jpn. J. Appl. Phys., Part 1 40 (2001) 2173.
[3] T.Y. Bin, R.-S. Huang, Sens. Actuators 11 (1987) 1.
[4] H.-C. Lee, R.-S. Huang, IEEE Trans. Electron Dev. 39 (1992) 313.
[5] D. Nicolaescu, V. Filip, J. Itoh, F. Okuyama, J. Vac. Sci. Technol. B 18 (2000) 1078.
[6] R.-S. Huang, H.-C. Lee, M. Gross, C.M. Horwitz, Proc. SPIE 2101 (1993) 62.
[7] H.H. Busta, J.E. Pogemiller, B.J. Zimmerman, IEEE Trans. Electron Dev. 40 (1993) 1530.
[8] S.H. Xia, J. Liu, D.F. Cui, J.H. Han, S.F. Chen, L. Wang, J. Vac. Sci. Technol. B 15 (1997) 1573.
[9] C.A. Spindt, I. Brodie, L. Humphrey, E.R. Westerberg, J. Appl. Phys. 47 (1976) 5248–5263.
[10] N. Badi, K. He, A. Nair, A. Bensaoula, International Vacuum Nanoelectronics Conference, IVNC 2004, 2004, pp. 24–25.
[11] S. Timoshenko, S. Woinowsky-Krieger, Theory of plates and shells, McGraw-Hill, New York, 1959.
[12] J.Y. Pan, P. Lin, F. Maseeh, S.D. Senturia, Solid State Sensor and Actuator Workshop, Fourth Technical Digest, IEEE, June 1990.
[13] D. Nicolaescu, V. Filip, J. Itoh, F. Okuyama, Analysis of a pressure sensor using n-Si/nitrogen doped diamond cathodes, J. Vac. Sci. Technol. B18 (2000) 1077.
[14] N. Badi, A. Tempez, D. Starikov, A. Bensaoula, V.P. Ageev, A. Karabutov, M.V. Ugarov, V. Frolov, E. Loubnin, K. Waters, A. Shultz, Field emission from as-grown and surface modified BN and CN thin films, J. Vac. Sci. Technol. A 17 (1999) 1191.
[15] N. Badi, A. Tempez, J. Kulik, D. Starikov, N. Medelci, S.M. Klimentov, S.V. Garnov, V.P. Ageev, M.V. Ugarov, K. Water, A. shultz, A. Bensaoula, Boron nitride materials for tribological and high temperature high power devices, Mater. Res. Soc. Symp. Proc. 495 (1998) 359.